A fast physical optics method for the analysis of beam waveguides

Torsten Bondo[(1)] and Stig Busk Sørensen[(1)]

[(1)]*Ticra*
Læderstræde 34, DK-1201, Copenhagen
Email: ticra@ticra.com

INTRODUCTION

A fast physical optics (PO) method is presented which in two steps calculates the scattered field of an optical component in a beam waveguide (BWG). The first step involves a calculation of a set of equivalent currents on an auxiliary plane and the second step a field calculation from this current set.

The present work has been motivated by the major difficulties associated with accurate analysis of a complex BWG system at THz frequencies. One major difficulty is the use of components in the BWG that are large in wavelength. These components will make field calculation through the BWG using standard PO methods computationally time consuming. An immediate way to overcome this problem could be to apply ray-tracing techniques. However, for a complex BWG with many components, ray tracing is often inaccurate or impractical. Another way to overcome the problem could be to use Gauss-Laguerre beam expansion techniques. In many configurations [1] these techniques *do* provide fast and efficient ways to trace the beam.

However, the demands for a compact BWG system design forces some components to have a small *F/D* (focal length to diameter ratio). Since the Gaussian beam method is only accurate for large *F/D* [2] and does not account for beam truncation Gaussian beam techniques are not always sufficient.

The standard PO can be time consuming because of rapid phase variation of the currents in the integral. However, in a region where the beam is concentrated e.g., in the waist of a Gaussian beam or in the far field of a paraboloid, the PO integral is very fast to compute. Therefore, if an auxiliary plane is defined in a region where the beam is concentrated, the scattered field at any point in space can be found by employing two steps in the analysis: First, the field is calculated on the auxiliary plane and converted to equivalent currents on this plane. Secondly, the radiated field is calculated from the current distribution to an output plane or the next component.

As will be shown in the examples the method has the ability to overcome the rapid growth of computation time with frequency. Normally, the computation time for PO will increase with the frequency to the 4th power, whereas the computation time for the present method is nearly independent of the frequency. The price to pay for this speed of computation is a limited accuracy of the field outside the main beam determined by the truncation of the field by the auxiliary plane. If the size of this plane is increased the accuracy outside the centre of the beam is improved, but the computation time is also increased. The method has the further advantage of being very simple to implement. It is thus much simpler than frame based expansion techniques as suggested in [3] and [4].

It should be emphasized that the method is only applicable for a well-focused beam. If the field to be computed does not have a well-defined phase front and waist, the present method is not able to reduce the computation time.

ANALYSIS PROCEDURE

The procedure is illustrated in Figure 1. A feed is illuminating a reflector producing an approximate Gaussian beam. In the figure the waist of the beam and an output plane is indicated. It is assumed that the field from the reflector should be calculated on this plane where e.g. a subsequent optical component could be located. The standard PO procedure would be to calculate the induced electric currents $\overline{J}_e$ on the reflector using the PO approximation $\overline{J}_e = 2\hat{n}\times\overline{H}_i$, where $\hat{n}$ is the surface normal and $\overline{H}_i$ is the incident magnetic field from the feed. Hereafter, the field on the output plane is calculated by numerical integration of the radiated field from the currents. This procedure is accurate and also efficient if the size of the reflector is less than app. 50λ. If the frequency ν is increased the number of current elements on the reflector must also be increased such that the spacing in wavelengths is the same. This shows that the required number of current elements is proportional to ν^2. Similarly, the number of points on the output plane will normally also be proportional to ν^2 for obtaining a sufficiently close spacing for plotting or for calculating the incident field on the next optical component. Since the field from each current element must be calculated in each of the output points it is seen that the computational work becomes proportional to ν^4. This frequency dependency is clearly inconvenient for analysis of large reflectors.

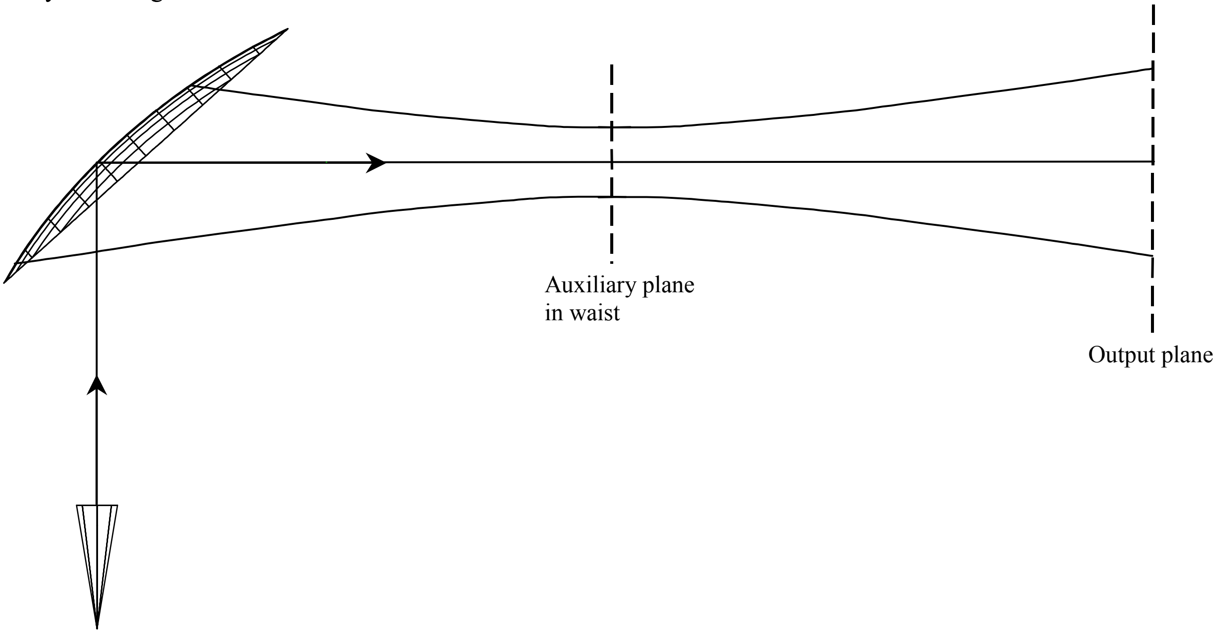

Figure 1. Offset ellipsoidal reflector with auxiliary plane and output plane after waist.

The computation time can be made nearly independent of the frequency by introducing an auxiliary plane through the waist as shown in Figure 1. On this plane the field can be computed very fast, because the field from each of the current elements on the reflector will have nearly the same phase. This means that the integrand in the PO-integral will be nearly constant, and that it can be accurately computed using only a small number of current elements on the reflector. The incident field on the auxiliary plane can be converted to equivalent currents radiating the same field as the currents on the reflector in the half space to the right of the plane. From the equivalence principle it can be shown [5], that each of the following three sets of currents

$$\overline{J}_e = \hat{n} \times \overline{H}, \qquad \overline{J}_m = -\hat{n} \times \overline{E} \tag{1}$$

$$\overline{J}_e = 2\hat{n} \times \overline{H} \tag{2}$$

$$\overline{J}_m = -2\hat{n} \times \overline{E}\,, \tag{3}$$

will radiate the correct field to the right of the auxiliary plane. Here $\overline{E}$ and $\overline{H}$ are the incident fields on the plane and $\hat{n}$ is the normal vector of the plane, pointing to the right. In (1) the equivalent currents consist of both electric and magnetic currents, whereas in (2) and (3) only one of the types are used. Each of the three sets of equivalent currents will exactly radiate the scattered field from the reflector on the right side of the plane. One the left hand side (1) will give a zero field, and (2) and (3) will give a field which is the mirror of the field on the right hand side.

If the desired output plane is located to the left of the auxiliary plane as shown in Figure 2, the described procedure cannot immediately be used because the currents (1), (2) and (3), do not radiate the field from the reflector to the right of the auxiliary plane. This can, however, be remedied simply by using the advanced potential instead of the usual retarded potential in the radiation integrals. The electric vector potential $\overline{A}_e$ is a solution to the differential equation

$$(\nabla^2 + k^2)\overline{A}_e = -\mu \overline{J}_e\ , \tag{4}$$

where $k=2\pi/\lambda$ is the wavenumber, μ is the permeability and $\overline{J}_e$ is the electric currents on the auxiliary plane. The standard solution to (4) is given by

$$\overline{A}_e = \frac{\mu}{4\pi} \iint_{aux.} \overline{J}_e \frac{e^{-jkR}}{R} ds' \ , \tag{5}$$

where the integration is performed over the currents on the auxiliary plane, ds' is the surface element on the plane and $R = |\overline{r} - \overline{r}'|$ is the distance from the current element to the observation point $\overline{r}$ on the output plane. The factor e^{-jkR}/R is denoted the retarded potential because it relates the radiated field to the currents delayed by the time R/c, (c = speed of light). Another solution to (4) is given by

$$\overline{A}_e = \frac{\mu}{4\pi} \iint_{aux.} \overline{J}_e \frac{e^{+jkR}}{R} ds' \ , \tag{6}$$

where e^{+jkR}/R is denoted the advanced potential because the field is in advance of the source. The usual radiation condition by which the field must be outwards propagating is not fulfilled by (6). Here the field converges towards the source and (6) is thus a non-physical solution to (4). For both potentials the corresponding electric and magnetic fields can be found from [5]

$$\overline{E} = -j\omega \left(\overline{A}_e + \frac{1}{k^2} \nabla (\nabla \cdot \overline{A}_e) \right) \tag{7}$$

$$\overline{H} = \frac{1}{\mu} \nabla \times \overline{A}_e . \tag{8}$$

The radiation from the magnetic currents can be computed in a similar way by a retarded and an advanced potential. In the situation shown in Figure (2) the advanced potential is very useful because the currents (1), (2) and (3) will then radiate the incident field to the left of the auxiliary plane. This can be proved by considering a plane wave as the incident field on the auxiliary plane. From the known radiation by the currents (1)-(3) to the right of the auxiliary plane using the retarded potential, it is easy to show that the same currents with the advanced potential will radiate the incident plane wave to the left of the auxiliary plane. Since an arbitrary incident field can be expanded in a spectrum of plane waves, it is seen that the field to the left of the plane can be reproduced by the equivalent currents using the advanced potential. In this way the incident field can be reconstructed on output planes parallel to the auxiliary plane as long as the output plane does not intersect the reflector.

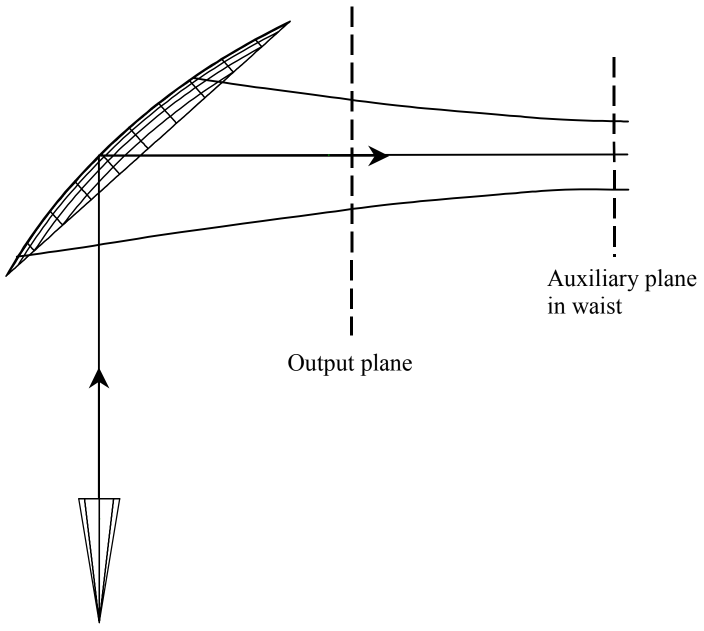

Figure 2. Output plane before waist.

OPTIMUM POSITION OF THE AUXILIARY PLANE

It is interesting to know the optimum position of an auxiliary plane and in which cases it will reduce the computation time. To answer this question we consider the Gaussian beam in Figure 3.

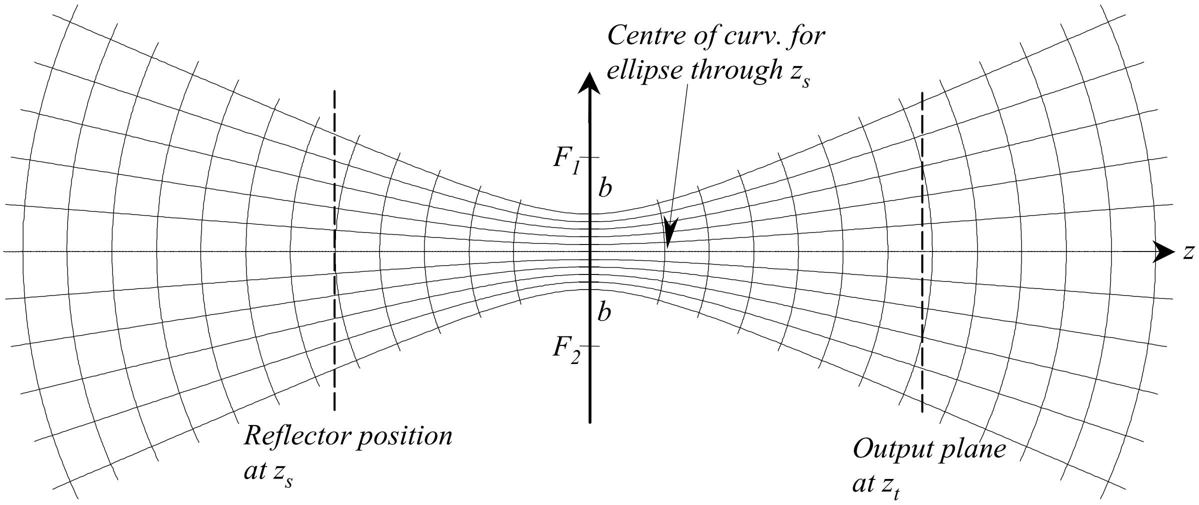

Fig. 3. Gaussian beam

The two points, F_1 and F_2, are located the distance b from the beam axis. It can be shown that the surfaces of constant phase are ellipsoids, which in the cut of the figure are ellipses with focal points F_1 and F_2. The ellipsoids are obtained by rotating the figure around the z-axis. The orthogonal curves in the figure (hyperbolas with the same foci) represent surfaces of constant amplitude. If the reflector generating the Gaussian beam is located at z_s as indicated in the figure, the reflector could be replaced by a set of currents with constant phase on the ellipsoid passing through the centre of the reflector. The radiation from these currents will add up in nearly constant phase on the output plane located at the centre of curvature of the ellipsoid. This plane is therefore the output plane on which the PO currents on the reflector can most easily be integrated. When the reflector is located at z_s the curvature of the beam at the centre of the reflector becomes

$$R = z_s(1 + b^2 / z_s^2) \tag{9}$$

by the usual Gaussian beam formula [6]. The centre of curvature of the ellipsoid will thus be located at

$$z_s - R = -b^2 / z_s \tag{10}$$

which is the optimum position of the output plane. The distance b is related to the waist size w_o by $w_o = \sqrt{2b/k}$. From consideration of the distances from points on an ellipsoid of equal phase to points on an output plane, it can be shown that the minimum number of PO current elements n_p on a reflector located at the ellipsoid can be estimated by

$$n_p(s,t) \cong \alpha^2 \beta^2 \frac{(1+s^2)(1+t^2)}{(t-s)^2} \ . \tag{11}$$

In this equation s is related to the position of the reflector by $s = z_s / b$ and t is related to the position of the output plane z_t by $t = z_t / b$. The constants α and β specify the sizes of the reflector and output plane, respectively, such that the field down to $\exp(-\alpha^2)$ will be covered by the reflector and down to $\exp(-\beta^2)$ for the output plane. It is seen that if the position of the output plane is chosen according to (10) we have $t = -1/s$ resulting in the minimum value $\alpha^2 \beta^2$ of (11). The PO integration procedure is based on the Gauss-Legendre integration rule and is described in detail in [7]. The computation time for calculating the field from the reflector in n_o points on the output plane becomes proportional to the number of connections to be made between points on the reflector and points on the output plane. For the direct PO integration this will give

$$N_{dir} = n_p(s,t)\, n_o \ . \tag{12}$$

If an auxiliary plane located at z_a is used the computation time will become proportional to

$$N_{aux} = n_p(s,a)\, n_p(a,t) + n_p(a,t)\, n_o \ , \tag{13}$$

where $a = z_a / b$ is the position of the auxiliary plane. In a practical case the output plane could be a second reflector and if it is assumed that the necessary number of current elements on the second reflector is equal to the number of current elements on the first, it is seen that

$$N_{dir} = n_p^2(s,t) \tag{14}$$

$$N_{aux} = 2n_p(s,a)\, n_p(a,t) \ . \tag{15}$$

In (15), a should be chosen to minimise N_{aux}. This value of a can be found analytically using (11). Some results (normalised by $\alpha^4 \beta^4$) with the direct and the auxiliary plane method are shown in Figure 4 and 5. In Figure 4 the reflector is located at s=-5, and the output plane varies from z/b=-5 to 10. It is seen that the direct method is efficient if the output plane is close to the waist, whereas the auxiliary-plane procedure is efficient at some distance from the waist. In Figure 5 the reflector is (a plane mirror) located exactly at the waist t=0, and it is seen that the direct method is good far away from the waist, whereas the auxiliary-plane procedure is efficient close to the waist. In general it can be shown, that if one of the equations (14) and (15) gives a large number the other will give a small number, such that the PO calculations can be done efficiently for all positions of the output plane.

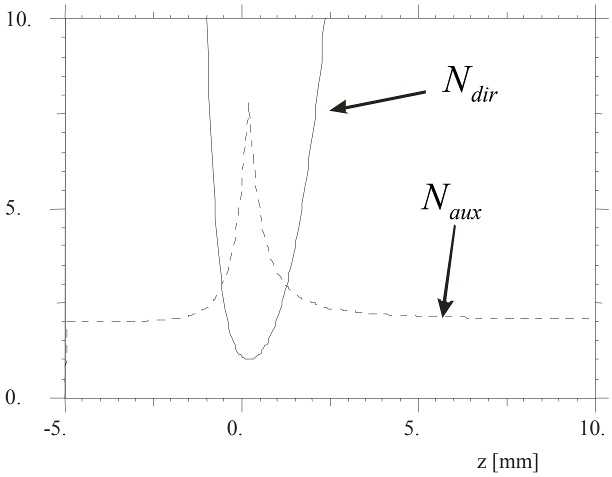

Fig. 4. Direct vs. aux. plane for s=-5

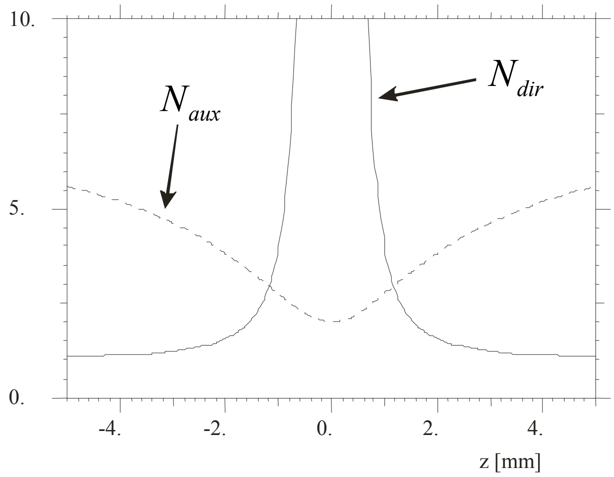

Fig. 5. Direct vs. aux. plane for s=0

OFFSET ELLIPSOIDAL REFLECTOR EXAMPLE

An offset ellipsoidal reflector as shown in Figure 6 is used as an example to test the auxiliary-plane procedure. The angle of incidence on the reflector is 45° and the rim of the reflector is defined by the intersection of a cone with half opening angle 21° and apex in the focal point on the negative x-axis. The reflector is illuminated by a Gaussian beam and analysed at the two frequencies λ=0.9 mm and λ=0.09 mm. For both frequencies the electric field is polarised in the plane of symmetry and the taper on the reflector is approximately -60 dB. The reflector is an ellipsoid with one focal point at x=-63.5 mm and the other focal point at z=104 mm in the coordinate system shown in the figure. The reflected beam has its waist at z=88.8 mm and b=36.0 mm for λ=0.9 mm. For λ=0.09 mm the waist is located at z=103.8 mm with b=4.0 mm.

In the following figures the radiated field from the reflector in the plane of symmetry is shown. The field at the waist is shown in Figures 7-8. The auxiliary plane is located at the waist and truncated at ±15 mm and ±2 mm for λ=0.9 mm and λ=0.09 mm, respectively. In Figures 9-10 the direct and auxiliary-plane methods are compared for λ=0.9 mm at the distances z=240 mm and z=40 mm. The distance z=40 mm is to the left of the waist so that the retarded potential must be used in the auxiliary-plane method. In Figures 11-12 the analysis is repeated for λ=0.09 mm. It is seen that the main beam is computed with good accuracy by the auxiliary-plane method down to approximately 80 dB below the beam maximum. A similar accuracy has been found for the field in the plane orthogonal to the plane of symmetry and for the cross polarisation. The accuracy can be improved by using a larger auxiliary plane (i.e. less truncation of the field in the waist), but this will also increase the computation time. If all the small diffraction ripples present in the direct analysis should be accurately calculated by the auxiliary-plane method, the plane should be considerably extended and there would be no saving of computation time compared to the direct method. In Table 1 and 2 the computational work is compared for the two methods with the No. of connections computed by (12) and (13). On an 800 MHz PC one connection can be computed in approximately 2μ sec. It is seen that the time saving is considerable for the new method and that the computation time is nearly independent of the frequency. The proposed method is thus especially attractive for output planes close to the reflector and for short wavelengths.

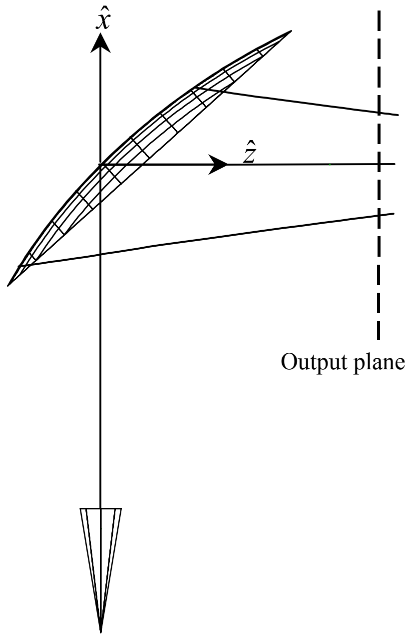

Figure 6
Geometry and coordinate system of offset reflector.

If the beam from the reflector is focused in the far field, the optimum position of the auxiliary plane will be in the far field. In this case the far field computed in a suitable integration grid can be considered as an expansion of the near field in a spectrum of plane waves. Integration of this spectrum of plane waves on an output plane in the near field will give a similar reduction in computation time as in the example described above. This means that the auxiliary plane method can be used for mirrors with a paraboloid surface equally well. In beam waveguides mirrors as well as other optical components such as lenses, FSS filters and apertures are present. It is important to note that the auxiliary plane method is not only restricted to field propagation from mirrors but can also be used for field propagation through all the above-mentioned components. The analysis of such components will be addressed in future papers.

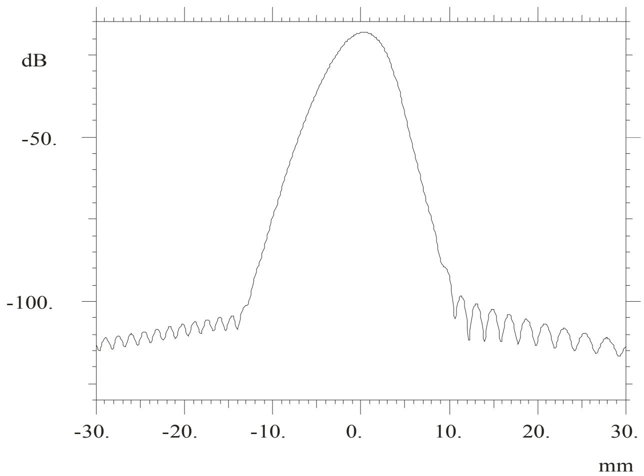

Figure 7 Waist field by the direct method λ=0.9 mm.

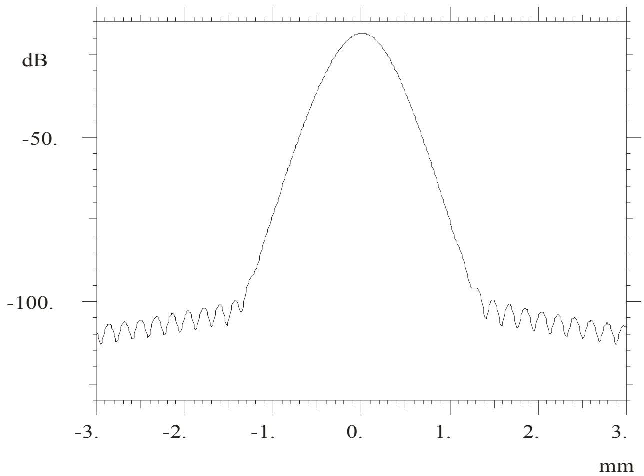

Figure 8 Waist field by the direct method λ=0.09 mm.

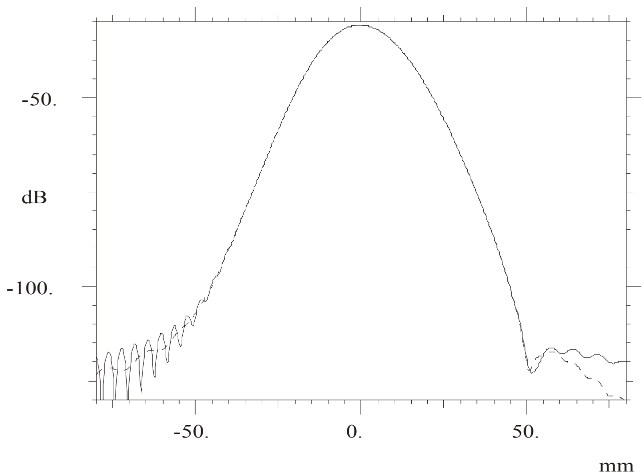

Figure 9 Field at z=240 mm, λ=0.9 mm.
Full line: direct method. Dashed line: aux. plane.

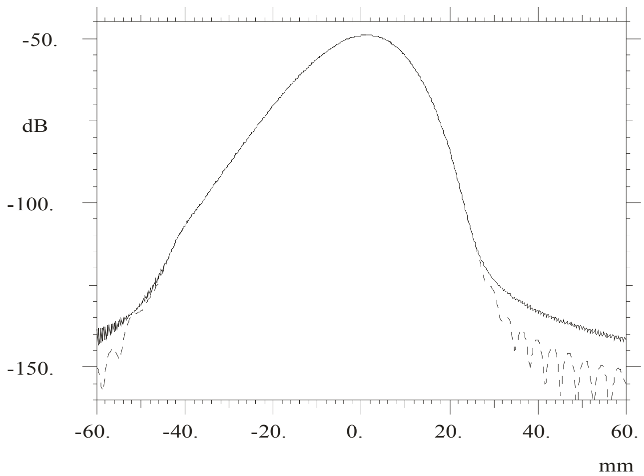

Figure 10 Field at z=240 mm, λ=0.09 mm.
Full line: direct method. Dashed line: aux. plane.

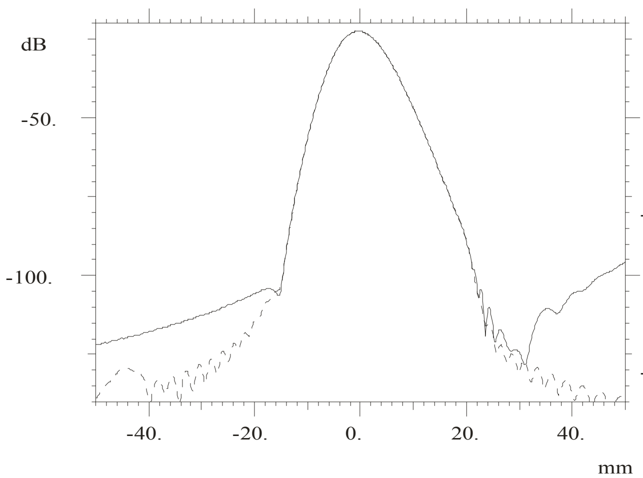

Figure 11 Field at z=40 mm, λ=0.9 mm.
Full line: direct method. Dashed line: aux. plane.

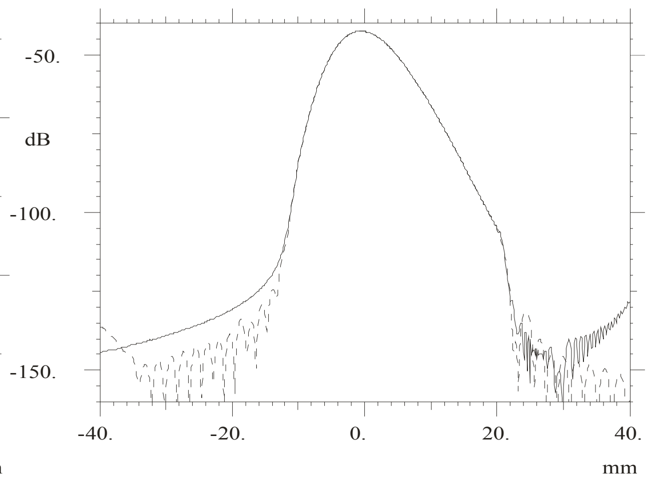

Figure 12 Field at z=40 mm, λ=0.09 mm.
Full line: direct method. Dashed line: aux. plane.

λ in mm	z in mm	Reflector points	Connections for 1000 output points in millions
0.9	240	2832	2.83
0.9	40	22798	22.80
0.09	240	81051	81.05
0.09	40	1115388	1115.39

Table 1 Number of current elements for direct integration.

λ in mm	z in mm	Reflector points	Aux. points	Connections for 1000 output points in millions
0.9	240	1403	1403	3.37
0.9	40	1403	1806	4.34
0.09	240	1403	1403	3.37
0.09	40	1403	1806	4.34

Table 2 Number of current elements for the auxiliary-plane procedure.

CONCLUSION

A procedure has been described for improving the speed of the classical Physical Optics method when applied to the analysis of beam waveguides. The procedure is very simple and involves the calculation of a set of equivalent currents on an auxiliary plane. It is expected that the procedure can be an alternative to the higher order Gaussian beam analysis often used for analysis of beam waveguides.

REFERENCES

[1] W.A. Imbriale and D.J. Hoppe, "Recent Trends in the Analysis of Quasioptical systems", *Proceedings from AP2000, Davos, Switzerland.*, April 2000.

[2] J. Tuovinen et al., "Near-field Analysis of a Thick Lens and Horn Combination: Theory and Measurements", *IEEE Transactions on Antennas and Propagation,* vol. 40, No. 6, June 1996.

[3] C. Rieckmann, M.R. Rayner and C. Parini, "Diffracted Gaussian beam analysis of quasi-optical multi-reflector systems", *Proceedings from AP2000, Davos, Switzerland.*, April 2000.

[4] T. Bondo and S.B. Sørensen, "Quasi-optical beam waveguide analysis using frame based Gaussin beam expansion", *Proceedings from 13th International Symposium on Space Terahertz Technology, Cambridge MA, USA*, March 2002.

[5] R.E. Collin and F.J. Zucker, "Antenna Theory Part 1", Chapter 1, McGraw-Hill Book Company, New York, 1969.

[6] P.F. Goldsmith, "Quasioptical Systems", *IEEE Press,* 1998

[7] K. Pontoppidan, "Technical Description of Grasp8", Ticra, March 2002, can be downloaded from www.ticra.com.